Dean&Francis
ISSN 2959-409X

MS003482

The effect of gelatin methatcryloyl (GelMA) on adipose-derived stem cells transplantation and wound healing

Yiwen Zhao

Beijing National Day School

Abstract:

Adipose-derived mesenchymal stem cells (ADSCs) are promising candidates for wound healing. To retain stem cells and ensure cells' function at the wound site, we use 3D scaffolds that mimic the extracellular matrix (ECM) to load ADSCs. Gelatin methacryloyl (GelMA) is a commonly used bioink to construct the 3D scaffold through extrusion-based 3D bioprinting. The study conducted various experiments to investigate the effectiveness of the ADSCs-GelMA hydrogel system with a different degree of methacrylate substitution. As a result, we found that GelMA hydrogel has a great ability to absorb water, maintain the viability and attachment of rats ADSCs (rADSCs), increase wound healing efficiency, etc. In addition, the hydrogel prepared by GelMA 50%-60% methacrylate substitution exhibited higher bioactivity than its 80%-90% counterparts. Therefore, the study not only proved the potential of GelMA hydrogel but also provided GelMA materials with a specific concentration of methacrylate substitution that further research could study and improve on.

Keywords: adipose-derived mesenchymal stem cells (ADSCs), wound healing, gelatin methacryloyl (GelMA), extrusion-based 3D bioprinting, 3D scaffold

1. Introduction

Wounds can be devastating for patients, strongly affecting people's health and daily life. Normally, skin can repair itself spontaneously through four stages: hemostasis, inflammation, proliferation, and maturation. Nonetheless, the healing process of extensive damage, such as burning wounds, might take a long time, or it may halt induced chronic wounds, like the wound of diabetes. Therefore, methods that promote wound healing are extensively studied in research. Debridement, skin grafts, and skin flaps are conventional surgical wound treatments, and non-surgical therapy involves wound dressings, topical formulations, scaffolds/hydrogels-based skin grafts, and skin substitutes. These methods have limited effects or shortcomings[1].

In recent years, many edge-cutting technologies have

ISSN 2959-409X

shown great promise in curing either acute or chronic wounds, and the application of stem cells has demonstrated an especially promising potential because they can function in all four phases of wound healing[1]. Compared with embryonic stem cells and induced pluripotent stem cells, mesenchymal stem cells (MSCs) possess many advantageous characteristics: they are immunosuppressive via paracrine signaling; they can regulate the activity of other cells and molecules that promote wound healing[2]. Adipose-derived MSCs (ADSCs) are found to be most effective. Specifically, ADSCs have a high availability, migration rate, the potential to multiple differentiate ability, and can secrete cytokines, immunomodulatory factors, and molecules that facilitate extracellular matrix construction, and these features were proved to be effective for wound healing in vivo experiments[3]. Nevertheless, survival and viability during the transplantation of stem cells are still problems, and there are two main strategies to solve this. One strategy is the genetic modification of stem cells, but it confronts risks like apoptosis and tumorigenesis in induced pluripotent stem cells[3]. Hence, the study will focus on the second strategy to improve the efficiency of stem cell therapy: delivering the cells with a 3D scaffold matrix[1]. Researchers found that hydrogels' high cytocompatibility provides a stable microenvironment for rADSCs to proliferate, and hydrogel composed of single natural polymers could adhere well to tissues, which increases the retention time of stem cells at wound sites[4,5]. The problems of poor control over the structure and insufficient biological capacity to sustain cells still exist for hydrogel[6].

Therefore, three-dimensional bioprinting, based on pre-programmed structures, can use biomaterials and living cells (bioink) to build 3D structures, such as tissue, organs, models, and scaffolds with improved control over the architecture[7]. The study used the most widely used extrusion-based 3D bioprinting. The selection of bioink is also crucial for the functionality of scaffolds, which must possess mechanical robustness and stability to maintain the structure and fidelity during bioprinting, as well as chemical tolerability, high biocompatibility, and biodegradability[8]. In this way, gelatin is a commonly used hydrogel[9]. For extrusion-based bioprinting specifically, the materials also need to possess gelation and shear-thinning properties[10]. Gelatin methacryloyl (GelMA) hydrogels improved the mechanical properties of pure gelatin, having suitable mechanical properties and biocompatibility for the growth of rADSCs[11].

Herein, the study will apply extrusion-based 3D bioprinting to construct a scaffold with GelMA hydrogel to load rADSCs, investigating the function of the scaffold, the viability of rADSCs, and the system's effect on wound healing. Experiments in this study involve 5% $GelMA_M$ hydrogel (50%-60% methacrylate substitutions) and 5% $GelMA_H$ hydrogel (80%-90% methacrylate substitutions). The experiment accomplishes bioink's preparation, characterization of bioinks, bioactivity evaluation of rADSCs, printing property assessment, and the evaluation of healing results. It is hypothesized that this system will demonstrate an increased wound healing rate and a better healing effect.

2. Material and Methods

2.1 Material

Type B gelatin (240 bloom), methacrylic anhydride, Lithium Phenyl(2,4,6- trimethylbenzoyl)phosphinate (LAP) was purchased from Aladdin (Shanghai, China). Dialysis bags (MWCO 3500), CCK8 kit, calcein AM-PI, and FITC Phalloidin was purchased from Solarbio (Beijing, China).

2.2 rADSCs' separation and culture

Prepare α-MEM complete culture medium with 94% α-MEM basic medium, 5% serum-free medium, 1% Penicillin-Streptomycin (double antibody). Prepare 0.3% type I collagenase. Transfer 20 ml adipose tissue suspension and 10 mL 0.3% type I collagenase to each 50 mL centrifuge tube. Put the tube into a thermostatic shaker for 3 hours, and set the temperature as 37°C, and rotary speed at 90 rpm. After the digestion, add another 15 mL of α-MEM complete culture medium to each centrifuge tube to terminate digestion. Filter and collect the obtained tissue fluid through a 100 μm sieve, centrifuge at 1400 rpm for 5 minutes at room temperature, and discard the supernatant after completion. Then, 10 mL of α-MEM complete culture medium was again added to resuspend the cells at the bottom of the centrifuge tube and repeated the cleaning step once. Finally, 10 mL of α-MEM complete culture medium was added again to resuspend the cells. The resulting cell suspension was filtered using a 70 μm sieve and seeded in a 100 mm culture dish. Finally, it was transferred to a 37 ^{o}C incubator. Cells should be used before the 7th passage.

2.3 Synthesis of GelMA

20 g of gelatin was dissolved in 200 mL of deionized water at 50 °C. Then, 6 g of methacrylic anhydride for $GelMA_M$ and 14 g of methacrylic anhydride for $GelMA_H$ were added to the mixture dropwise under vigorous stirring. The reaction was continued at 50 °C[12]. After 4 hours, the mixture was purified through a dialysis bag, freeze-dried at -80 ^{o}C for 3 days, and then stored at -20 ^{o}C.

2.4 Characterization evaluation

2.4.1 Curing time evaluation

500 μL 5% GelMA with 0.1% LAP in a 2 mL vial was exposed to the blue light (405 nm) of 10 mW/cm^2, 20 mW/cm^2, and 25 mW/cm^2. The vials were inverted every second until no obvious fluid flow was observed.

2.4.2 Water content evaluation

The mass of a centrifuge tube M_0 and the mass of the centrifuge tube with 500 μL of 5% GelMA hydrogel in it were weighed. Freeze dried and weighed the mass of the tube and the dry weight of GelMA hydrogel. The water content was calculated using the following equation: [Eq-1]

$$Watercontent(\%) = \frac{(M_1 - M_0) - (M_2 - M_0)}{M_1 - M_0} \times 100,$$

where M_0 is the mass of the centrifuge tube, M_1 is the mass of the centrifuge tube and the wet weight of 500 μL of 5% GelMA hydrogel, and M_2 is the mass of the centrifuge tube and the dry weight of 500 μL of 5% GelMA hydrogel.

2.4.3 Water retention evaluation

The mass of the centrifuge tube was weighed. 200 μL 5% GelMA hydrogel with 0.2% LAP were added into centrifuge tubes. The total mass of GelMA hydrogel and the tube was weighed. The tube was centrifuged at 5000rpm for 5, 10, 20, 30 minutes. The water in the tube was removed with filter paper, and the total mass of the content and the tube was weighed. The water retention was calculated using the following equation: [Eq-2]

$$waterretention(\%) = \frac{M_2 - M_0}{M_1 - M_0} \times 100,$$

where M_0 is the mass of a centrifuge tube, M_1 is the initial mass of GelMA hydrogel and the centrifuge tube before centrifuge, and M_2 is the final mass of GelMA hydrogel and the centrifuge tube after centrifuge.

2.4.4 Gel fraction evaluation

The 5% GelMA hydrogel was first freeze-dried and weighed. The dried hydrogel was incubated in DI water for 6 hours. Afterward, the sample was freeze-dried and weighed. The gel fraction was calculated using the following equation: [Eq-3][12]

$$gelfraction(\%) = \frac{M_2}{M_1} \times 100,$$

where M_1 is the initial mass of the dried 5% GelMA hydrogel, and M_2 is the final mass of the dried 5% GelMA hydrogel after being incubated in DI water.

2.5 Cytocompatibility and biocompatibility evaluation

2.5.1 Extraction fluid culture and live/dead cell staining

100 μL of α-MEM complete culture medium that contains rADSCs with a concentration of 1x10^5 rADSCs/mL was added to a 96-well plate and cultured for 24 hours to ensure cell attachment. The extracting solution of hydrogel was obtained by incubation of the hydrogel in DMEM medium (1:10 wt/v) for 3 days. The α-MEM complete culture medium was removed, and 150 μL extracting fluids were added. After being incubated for 48 hours, the cells in each well were washed with PBS, and stained by live/dead staining according to the manufacturer's instructions. A fluorescence confocal microscope was used to observe the fluorescence of live and dead cells[13].

2.5.2 CCK-8 test

100 μL of α-MEM complete culture medium that contains rADSCs with a concentration of 1x10^5 rADSCs/mL was added to a 96-well plate and cultured for 24 hours. The culture medium was removed from the wells of experimental groups, and 150 μL of GelMA extracts were added to the experimental groups. The culture medium in the control was replaced by 150 μL α-MEM complete culture medium. Then, rADSCs are cultured at 37 °C and 5% CO_2 for 24 hours. The cell viability of rADSCs was evaluated by a CCK-8 assay and the absorbance at 450 nm was recorded. The cell viability was calculated according to: [Eq-4]

$$cellviability(\%) = \frac{OD_e - OD_s}{OD_c - OD_s} \times 100,$$

where OD_e is the opacity density of the experimental group, OD_c is the opacity density of the control, and OD_s is the standard opacity density of the well without rADSCs.

2.5.3 Surface seeding on skeleton staining

40 μL of 5% GelMA was irradiated with blue light for gelation at the bottom of a 96-well plate. 100 μL of rADSCs in α-MEM complete culture medium at a concentration of 1x10^5 cells/mL were added to it and incubated for 24 hours. The cell cytoskeleton was stained with FlTC labeled phalloidin according to the manufacturer's instructions and observed by a fluorescence confocal microscope.

2.5.4 Cell encapsulation and live/dead cell staining

The rADSCs were first mixed with 5% GelMA and 0.2% LAP at a concentration of 1x10^5 /mL. Then, 30 μL of the mixture was dropped into a 96-well plate and irradiated with blue light (405 nm, 25 mW/cm^2, 60 s) for gelation.

ISSN 2959-409X

After being cultured for 24 hours and 72 hours, the hydrogels were stained with AM (2 μg/mL, 37 °C, 15 min) and 5 μg/mL propidium iodide (5 μg/mL, 37 °C, 5 min), and fluorescence images were obtained from a fluorescence confocal microscope[12].

2.5.5 $GelMA_M$ ink 3D bioprinting scaffold with rADSCs and live/dead cell staining

The bioinks composed of 5% $GelMA_M$, 0.2% LAP, and rADSCs ($1x10^6$ /mL) were transferred to a syringe. The printing was performed by an extrusion-based bioprinter at 22 °C, 1.0 bar under a printing speed of 5 mm/s through a 23 G nozzle, and the sample was deposited onto a 4 °C platform and was exposed to 25 mW/cm^2 blue light. After being incubated for 24 hours and 72 hours, the scaffold was stained with AM (2 μg/mL, 37 °C, 15 min) and 5 μg/mL propidium iodide (5 μg/mL, 37 °C, 5 min), and the fluorescence images were obtained using a fluorescence confocal microscope[12].

2.6 Wound healing effect evaluation in vivo

Full thickness skin wound was created on the back of rats. They were treated with PBS, rADSCs, and rADSCs loaded on a 3D GelMA scaffold, respectively. Photos of the wounds were taken on day 0, day 3, day 5, and day 7. On day 7, the rats were sacrificed. The wound granulation tissues were fixed with 4% paraformaldehyde and were stained by H&E and Masson staining[13].

3. Results and discussion

3.1 Characterization

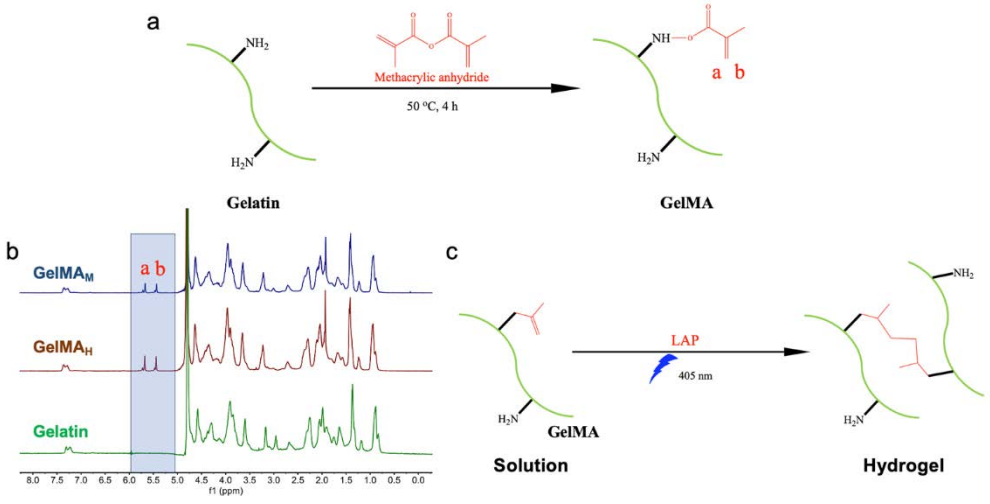

Figure 1. GelMA hydrogel synthesis.

(a)The mechanism of GelMA synthesis, (b) GelMA 1H nuclear magnetic resonance spectra (1H NMR), (c) GelMA blue light cross-linking curing.

At 50 °C, the methacryloyl groups were conjugated on the gelatin backbone by reacting with amine[14]. (figure 1. a) ^{1}H NMR of $GelMA_M$ and $GelMA_H$ have new peaks at ppm 5-6, which verified the introduction of double bonds on the gelatin backbone. The higher intensity at ppm 5-6 of $GelMA_H$ indicates the higher degree of methacryloyl substitution in $GelMA_H$. (figure 1. b) Covalent crosslinking of GelMA is formed under blue light exposure with the presence of photoinitiator LAP. (figure 1. c) By reacting gelatin with methacrylic anhydride, GelMA can be synthesized and photo crosslinked into a stable hydrogel at physiological temperatures. A study also shows that GelMA has high printability, and biocompatibility, which makes it a good material for 3D scaffolds[15].

Although the degree of methacrylate groups within 20% to 80% is capable of creating GelMA hydrogels with stable mechanical properties, the GelMA hydrogel has different characteristics when the degree of methacrylate groups varies[16]. The curing time of $GelMA_M$ and $GelMA_H$ decreases as the power of blue light increases from 10 mW/cm^2 to 25mW/cm^2, and the difference is especially significant between $GelMA_M$ and $GelMA_H$. Under constant light power, the curing time of $GelMA_M$ is always longer than that of $GelMA_H$, which means that increasing the degree of methacrylate groups will increase the efficiency of GelMA curing. The results of curing time correspond with a finding that an elevated degree of substitution (DS) leads to better formability and mechanical properties of GelMA[17]. However, at 25 mW/cm^2 blue light, the difference between the curing time of $GelMA_M$ and $GelMA_H$ is not as significant as the difference when the power of light is relatively high, so the DS has less effect as the power of light increases. (figure 2. a) GelMA hydrogel's ability to

maintain water contributes a lot for wound healing since hydrated wound bed is crucial for tissue regeneration[18]. In the experiment, both $GelMA_M$ and $GelMA_H$ contained more than 90% water. (figure 2. b) $GelMA_M$ and $GelMA_H$ also demonstrate perfect water retention ability, hardly losing water after centrifugation. (figure 2. c) Gel fraction is the fraction of polymerized molecules converted from gelatin and MA. The gel fraction of GelMA is above 90%, suggesting the hydrogel network is well-cross-linked. (figure 2. d)

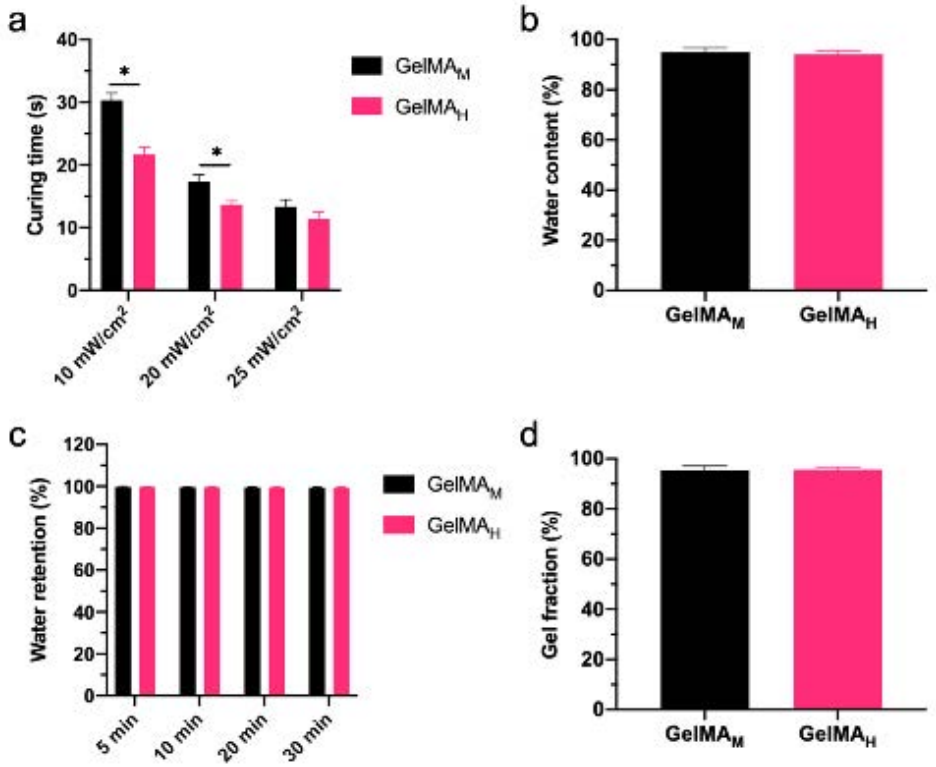

Figure 2. Characterization of GelMA bioinks. (a) GelMA hydrogel precursor solution (0.2% LAP) curing time under different blue light irradiation (b) Water content, (c) Water retention rate, (d) gel fraction. (n=3, *P<0.05)

3.2 Cytocompatibility and biocompatibility

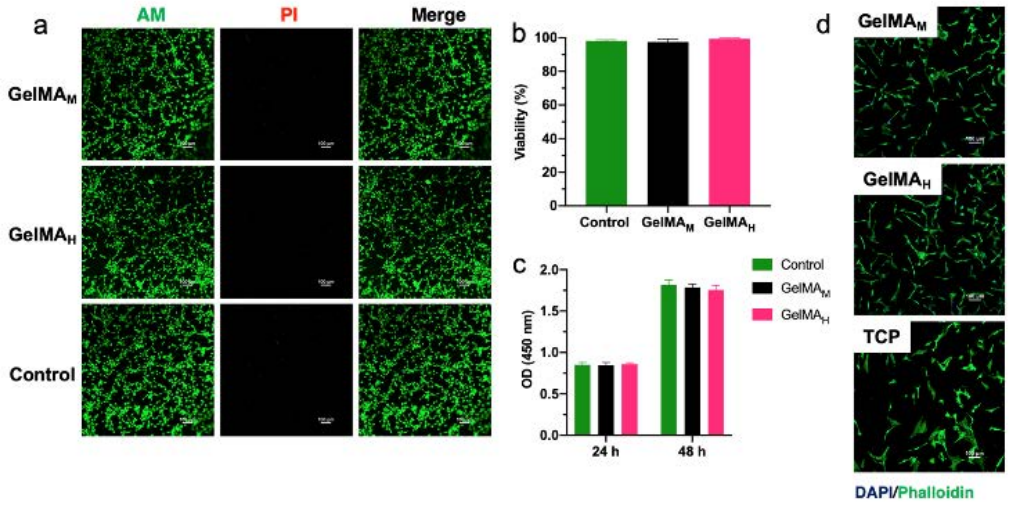

Figure 3. Biocompatibility evaluation of GelMA

ISSN 2959-409X

(a) live/dead staining of cell after 48-hour extraction solution culturing,
(b) statistics of viability, (c) CCK-8 test, (d) skeleton staining after 24-hour surface seeding, TCP: tissue culture plate (the control). (n=3)
In the fluorescence graph of live/dead cell staining, the amount of green fluorescence that labeled live cells outweighs the amount of red fluorescence that labeled dead cells in $GelMA_M$, $GelMA_H$, and the control. (figure 3. A) There isn't a significant difference between the viability of cells after 48 hours of culture in extracting fluid of $GelMA_M$ and $GelMA_H$ and the control, approaching 100%. (figure 3. a,b) Thus, rADSCs are able to survive well with the chemical content of GelMA. The increased opacity density in CCK-8 test indicates an increased number of cells in the sample due to cell proliferation. The absorbance of cells after the treatment of GelMA is similar to the control and increased with time, reflecting that the hydrogel has no cytotoxicity and no effect on cellular activity and proliferation. (figure 3. c) Phalloidin with green fluorescence dyes actin filaments in cells that can be used to view the cell morphology, and DAPI with blue fluorescence visualizes cell nuclei[19]. On solidified $GelMA_M$ and $GelMA_H$ hydrogels, the green fluorescence of cytoskeletons demonstrates that rADSCs attached and grew well after being implanted for 24 hours, indicating that the mechanical structure could support the attachment and migration of stem cells. (figure 3. d) Specifically, arginine-glycine-aspartic acid (RGD) and matrix metalloproteinase (MMP) motifs of gelatin mimic ECM, allowing cells to adhere, proliferate, and differentiate on and within the scaffold[17,20]. Also, the RGD sequences are unlikely to change because the reaction with MA only involves less than 5% of the amino acids, none of which contain RGD sequences[14].

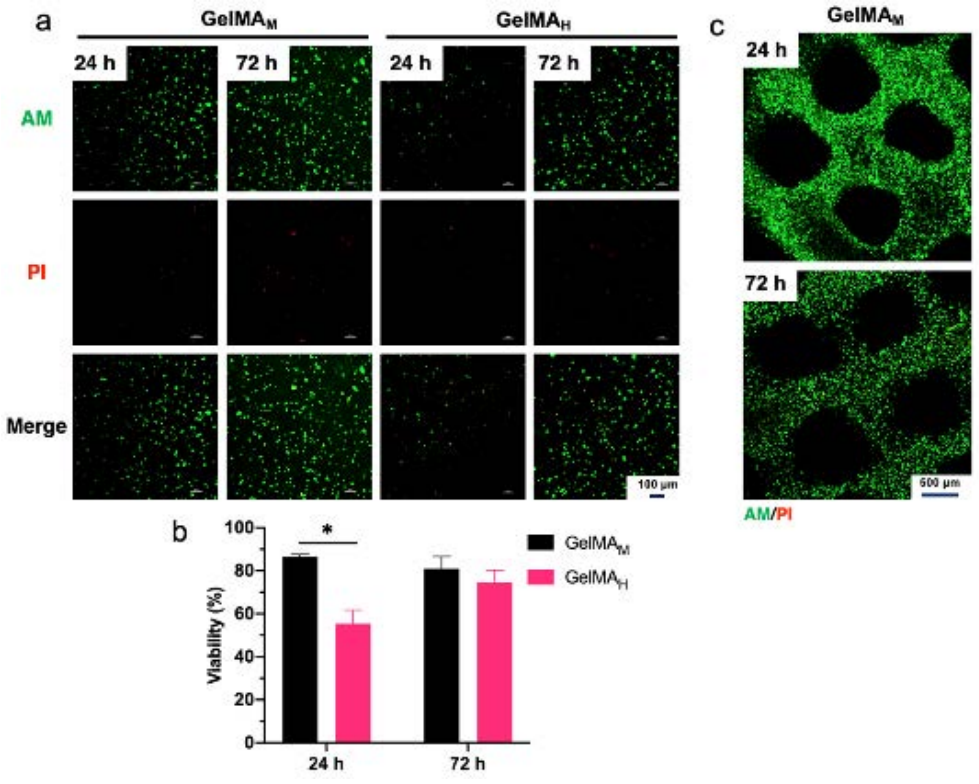

Figure 4. Cell viability evaluation on GelMA hydrogel.

(a) GelMA hydrogel wrapped rADSCs live/dead cell staining, (b) viability,
(c) live/dead cell staining of 3D bioprinted $GelMA_M$ bioink scaffold with rADSCs. (n=3, $*P<0.05$)
The viability of rADSCs varies when encapsulated in $GelMA_M$ and $GelMA_H$. After being cultured for 24 hours, 80%-90% of cells encapsulated in $GelMA_M$ survived, but only 50%-60% of cells encapsulated in $GelMA_H$ were viable. After three days, the viability of rADSCs encapsulated in both $GelMA_M$ and $GelMA_H$ falls between 80%-90%. (figure 4. ab) The high concentration of methacrylate groups might impede rADSCs in the short term. The

increasing viability after 72 hours might be due to cells elongating and migrating to form interconnected networks that are more stable than at the beginning[16]. Another explanation for increased viability may be because of individual differences among ADSCs that cause weaker cells to die within 24 hours and the cells with stronger viability to survive. Since the first three days are crucial for wound healing, $GelMA_M$ is determined to be a more effective hydrogel to treat wounds, and the study further evaluates $GelMA_M$'s biocompatibility during 3D printing. According to the graph from the fluorescence confocal microscope, the printing process doesn't impact the cells. There's hardly any red fluorescence that represents dead cells, so only a few cells died 24 hours and 72 hours after 3D bioprinting. (figure 4. c)

3.3 In vivo healing effect

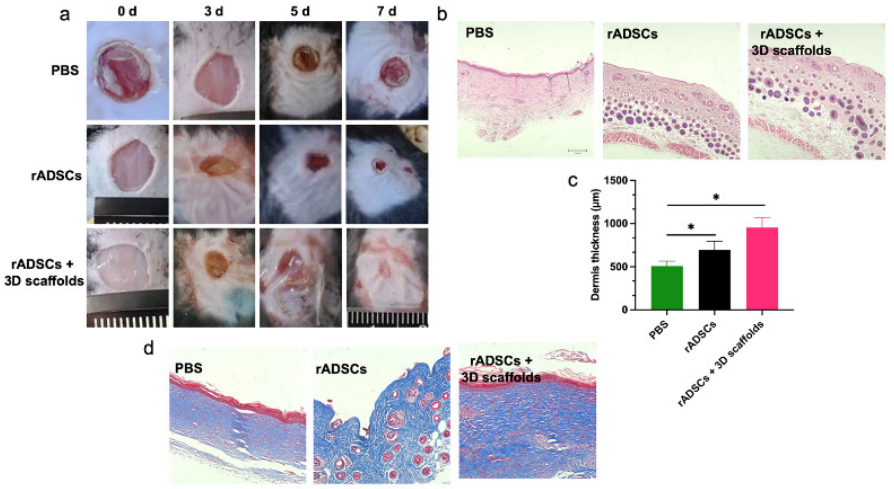

Figure 5. In vivo wound healing effect. (a) GelMA-loaded rADSCs cell printed scaffolds for the treatment of mouse skin injuries, and the wound morphology within 7 days, (b) HE staining, (c) the thickness of the dermis layer of the wound on day 7, (d) Masson staining. (n=3, *P<0.05)

Microscopically, the wound's surface area was smaller for rats that were treated with rADSCs and rADSCs + 3D scaffold on day 3. On day 7, the wound treated by rADSCs had a smaller area than the control, and the wound treated by rADSCs + 3D scaffold was cured to the greatest extent among the three rats, having the smallest wound surface and depth. (figure 5. a) While hair follicles and muscle layers aren't visible on the rats that were treated with PBS 7 days after being injured, rADSCs induced the formation of hair follicles and muscles in rats that were treated with rADSCs and rADSCs + 3D scaffolds. In addition, the apparently broader interstitial space represents better wound healing. (figure 5. b) Treating with rADSCs + 3D scaffolds improve the dermis thickness significantly compared with treating with rADSCs and not with treatment. (figure 5. c) In Masson staining, the collagen layer of rat's skin that is treated with rADSCs + 3D scaffolds is thicker than the skin without treatment, and unlike the rat that is treated with rADSCs, the collagen layer is more condensed while the epidermis is well developed. (figure 5. d) Since rADSCs are usually located in specific spaces where they are closely attached to ECM and other support cells, rADSCs suspension is insufficient to maintain the activity of rADSCs and promote rADSCs working at wound sites[17]. In contrast, the GelMA 3D scaffold functions as the ECM, constructing a desirable microenvironment for rADSCs to attach, migrate, and differentiate. So, the 3D scaffold enhanced the curing effect and efficiency of rADSCs at the wound site.

Above all, the study's results accord with various credible studies[17,18]. Nonetheless, the study has some disadvantages and a large space to improve. The most important stem cell characteristic for wound healing is differentiation, while the study only investigated the growth and the number of ADSCs. So GelMA hydrogel's influence on cells differentiation can be an investigating direction in future research. Moreover, in vivo experiments, the mechanism of rADSCs+3D scaffolds healing wounds needs more evidence to substantiate because the improved healing effect may simply be due to the addition of 3D scaffolds instead of its support for rADSCs. Thus, a further experiment should manipulate a positive control with only a 3D scaffold and statistically compare whether the effect of the rADSCs+3D scaffold group exceeds the total effect of the rADSCs group plus the 3D scaffold group.

The GelMA -ADSCs system can also be used in different

ISSN 2959-409X

kinds of wounds other than the acute wound models. GelMA and rADSCs collected under hypoxia conditions are able to accelerate angiogenesis at the wound site on aged skin, which is generally harder to cure than young skin[21]. Another research suggests that burning wounds can be improved on a rADSCs loaded by 3D bioprinted scaffold, so GelMA might further increase the effectiveness of rADSCs on burning wounds considering its high biocompatibility demonstrated in this study[22]. Many studies also investigated effective modifications on GelMA. Curcumin-incorporated 3D-printed GelMA increases rADSCs' viability in wounds and promotes diabetic wound healing in vivo[11].

4. Conclusion

The study presents experiments on the physical, chemical, and biological properties of 5% GelMA. $GelMA_M$ and $GelMA_H$ demonstrate similarly high abilities to maintain moisture and have low cytotoxicity. However, $GelMA_M$ is considered to be more appropriate for treating wounds because of the significantly higher biocompatibility when encapsulating rADSCs. As a result, the in vivo experiment substantiated that $GelMA_M$ hydrogel combined with rADSCs could promote wound healing more effectively and efficiently compared with pure stem cell treatments and the control.

References

[1] Kolimi, P., Narala, S., Nyavanandi, D., Youssef, A. A. A., & Dudhipala, N. (2022). Innovative Treatment Strategies to Accelerate Wound Healing: Trajectory and Recent Advancements. Cells, 11(15), 2439. https://doi.org/10.3390/cells11152439

[2] Lee, S. H., Jin, S. Y., Song, J. S., Seo, K. K., & Cho, K. H. (2012). Paracrine effects of adipose-derived stem cells on keratinocytes and dermal fibroblasts. Annals of dermatology, 24(2), 136–143. https://doi.org/10.5021/ad.2012.24.2.136

[3] Hassanshahi, A., Hassanshahi, M., Khabbazi, S., Hosseini-Khah, Z., Peymanfar, Y., Ghalamkari, S., Su, Y. W., & Xian, C. J. (2019). Adipose-derived stem cells for wound healing. Journal of cellular physiology, 234(6), 7903–7914. https://doi.org/10.1002/jcp.27922

[4] Xiao, X., Huang, Z., Jiang, X., Yang, Y., Yang, L., Yang, S., Niu, C., Xu, Y., & Feng, L. (2022). Facile synthesize of norbornene-hyaluronic acid to form hydrogel via thiol-norbornene reaction for biomedical application. Polymer, 245, 124696. https://doi.org/https://doi.org/10.1016/j.polymer.2022.124696

[5] Chen, J., Yang, J., Wang, L., Zhang, X., Heng, B. C., Wang, D. A., & Ge, Z. (2020). Modified hyaluronic acid hydrogels with chemical groups that facilitate adhesion to host tissues enhance cartilage regeneration. Bioactive materials, 6(6), 1689–1698. https://doi.org/10.1016/j.bioactmat.2020.11.020

[6] Omidian, H., & Chowdhury, S. D. (2023). Advancements and Applications of Injectable Hydrogel Composites in Biomedical Research and Therapy. Gels (Basel, Switzerland), 9(7), 533. https://doi.org/10.3390/gels9070533

[7] Dey, M., & Ozbolat, I. T. (2020). 3D bioprinting of cells, tissues and organs. Scientific reports, 10(1), 14023. https://doi.org/10.1038/s41598-020-70086-y

[8] Gungor-Ozkerim, P. S., , Inci, I., , Zhang, Y. S., , Khademhosseini, A., , & Dokmeci, M. R., (2018). Bioinks for 3D bioprinting: an overview. Biomaterials science, 6(5), 915–946. https://doi.org/10.1039/c7bm00765e

[9] Mad-Ali S., Benjakul S., Prodpran T., Maqsood S. Characteristics and gelling properties of gelatin from goat skin as affected by drying methods. J. Food Sci. Technol. 2017;54:1646–1654. doi: 10.1007/s13197-017-2597-5.

[10] Zhang, M., Zhang, C., Li, Z., Fu, X., & Huang, S. (2022). Advances in 3D skin bioprinting for wound healing and disease modeling. Regenerative biomaterials, 10, rbac105. https://doi.org/10.1093/rb/rbac105

[11] Xia, S., Weng, T., Jin, R., Yang, M., Yu, M., Zhang, W., Wang, X., & Han, C. (2022). Curcumin-incorporated 3D bioprinting gelatin methacryloyl hydrogel reduces reactive oxygen species-induced adipose-derived stem cell apoptosis and improves implanting survival in diabetic wounds. Burns & trauma, 10, tkac001. https://doi.org/10.1093/burnst/tkac001

[12] Xiao, X., Yang, Y., Lai, Y., Huang, Z., Li, C., Yang, S., Niu, C., Yang, L., & Feng, L. (2023). Customization of an Ultrafast Thiol-Norbornene Photo-Cross-Linkable Hyaluronic Acid-Gelatin Bioink for Extrusion-Based 3D Bioprinting. Biomacromolecules, 24(11), 5414–5427. https://doi.org/10.1021/acs.biomac.3c00887

[13] Zhang, Z., Guo, J., He, Y., Han, J., Chen, M., Zheng, Y., Zhang, S., Guo, S., Shi, X., & Yang, J. (2022). An injectable double network hydrogel with hemostasis and antibacterial activity for promoting multidrug-resistant bacteria infected wound healing. Biomaterials science, 10(12), 3268–3281. https://doi.org/10.1039/d2bm00347c

[14] Van Den Bulcke, A. I., Bogdanov, B., De Rooze, N., Schacht, E. H., Cornelissen, M., & Berghmans, H. (2000). Structural and rheological properties of methacrylamide modified gelatin hydrogels. Biomacromolecules, 1(1), 31–38. https://doi.org/10.1021/bm990017d

[15] Arguchinskaya, N. V., Isaeva, E. V., Kisel, A. A., Beketov, E. E., Lagoda, T. S., Baranovskii, D. S., Yakovleva, N. D., Demyashkin, G. A., Komarova, L. N., Astakhina, S. O., Shubin, N. E., Shegay, P. V., Ivanov, S. A., & Kaprin, A. D. (2023). Properties and Printability of the Synthesized Hydrogel Based on GelMA. International journal of molecular sciences, 24(3), 2121. https://doi.org/10.3390/ijms24032121

[16] Nichol, J. W., Koshy, S. T., Bae, H., Hwang, C. M., Yamanlar, S., & Khademhosseini, A. (2010). Cell-laden microengineered gelatin methacrylate hydrogels. Biomaterials, 31(21), 5536–5544. https://doi.org/10.1016/j.biomaterials.2010.03.064

[17] Gautam, S., Dinda, A. K., & Mishra, N. C. (2013). Fabrication and characterization of PCL/gelatin composite nanofibrous scaffold for tissue engineering applications by electrospinning method. Materials science & engineering. C, Materials for biological applications, 33(3), 1228–1235. https://doi.org/10.1016/j.msec.2012.12.015

[18] Hoch, E., Schuh, C., Hirth, T., Tovar, G. E., & Borchers, K. (2012). Stiff gelatin hydrogels can be photo-chemically synthesized from low viscous gelatin solutions using molecularly functionalized gelatin with a high degree of methacrylation. Journal of materials science. Materials in medicine, 23(11), 2607–2617. https://doi.org/10.1007/s10856-012-4731-2

[19] Romani, M., & Auwerx, J. (2021). Phalloidin Staining of Actin Filaments for Visualization of Muscle Fibers in Caenorhabditis elegans. Bio-protocol, 11(19), e4183. https://doi.org/10.21769/BioProtoc.4183

[20] Yue, K., Trujillo-de Santiago, G., Alvarez, M. M., Tamayol, A., Annabi, N., & Khademhosseini, A. (2015). Synthesis, properties, and biomedical applications of gelatin methacryloyl (GelMA) hydrogels. Biomaterials, 73, 254–271. https://doi.org/10.1016/j.biomaterials.2015.08.045

[21] Li, S., Sun, J., Yang, J., Yang, Y., Ding, H., Yu, B., Ma, K., & Chen, M. (2023). Gelatin methacryloyl (GelMA) loaded with concentrated hypoxic pretreated adipose-derived mesenchymal stem cells(rADSCs) conditioned medium promotes wound healing and vascular regeneration in aged skin. Biomaterials research, 27(1), 11. https://doi.org/10.1186/s40824-023-00352-3

[22] Roshangar, L., Rad, J. S., Kheirjou, R., & Khosroshahi, A. F. (2021). Using 3D-bioprinting scaffold loaded with adipose-derived stem cells to burns wound healing. Journal of tissue engineering and regenerative medicine, 15(6), 546–555. https://doi.org/10.1002/term.3194